EGG-M-17987
CONF-870679--6

SENSING AND MODELLING OF GAS METAL ARC WELDING

H. B. Smartt, J. A. Johnson,
R. T. Allemeier, N. M. Carlson,
C. J. Einerson, A. D. Watkins

Idaho National Engineering Laboratory
EG&G Idaho, Inc.
P. O. Box 1625
Idaho Falls, Idaho 83415

DE89 011153

EGG-M--17987

ABSTRACT

Welding automation is normally concerned with directly controlling such factors as current, arc voltage, travel speed, and filler wire speed. Several other levels of control can be identified beyond present technology including control of weld heat input, cooling rate, and bead geometry (bead width, penetration, reinforcements, and defects). This work describes the development of a steady-state model of the gas metal arc (GMA) welding process which allows independent control of the heat and mass input to the base metal. An electro-optical technique for measurement of the welding pool and groove geometry is also described along with an ultrasonic method for sensing the weld bead.

INTRODUCTION

In simplest terms, the function of any fusion welding process is the input of heat and mass to the joint to be welded. The response of the material(s) being joined to these inputs (and any post-weld treatments) determines the state of the weld and thus its properties, which determine its suitability for the desired application. The objective of a rational arc welding procedure, then, should be to provide the appropriate heat and mass input to the weld which will result in the desired properties. Welding procedures are generally based on the allowable ranges of the critical parameters, and automation, if used at all, normally deals with direct control of factors such as current, arc voltage, travel speed, and metal deposition rate.

In recent years, there has been a significant growth in the use of mechanized welding systems. The most popular alternative process is gas metal arc (GMA) welding and its variants, especially for arc welding applications using robots. The GMA process as used today, however, is subject to the same fundamental limitations as virtually all arc welding processes. Control of the process is limited to those factors to which machine builders are accustomed, such as electrode wire speed, welding speed, current, and voltage. The factors that the welding engineer would like to control, such as reinforcement area, weld heat input, microstructure, and mechanical and physical properties of the weld, are not directly controllable except in isolated cases.

This work, in collaboration with related work at MIT, is an effort to develop the fundamental basis to independently control desired physical properties of the

---

weld. To achieve this goal, sensing and modelling of the physical processes occurring in GMA welding are required. Toward this end, three integrated research efforts are being conducted at the Idaho National Engineering Laboratory (INEL): 1) developing a real-time process control model, 2) developing and implementing a weld vision system, and 3) ultrasonic sensing of the weld bead.

GMA PROCESS MODEL

The model developed in this work is intended for use in welding thick section carbon or alloy steel in the spray transfer mode. The requirements of the model have been set somewhat arbitrarily at controlling the weld bead reinforcement area to within $\pm 5\%$, and controlling the weldment heat input per unit length of weld to $\pm 10\%$. These ranges are believed to be realistically achievable and usable. At this point, the model does not contain information regarding the formation, detachment, or transfer of the droplets from the electrode wire to the weld pool.

A set of six equations provides the basis for the model[1]:

(1) $H = EI\eta^*/R$	Heat input to the base metal
(2) $G = A_w S/R$	Reinforcement
(3) $E = E_o + nI$	Power supply characterization
(4) $IE = IV_w + IV_a$	Power balance
(5) $IV_w + \eta' IV = A_w \delta S H_m$	Power required to melt the wire
(6) $IV_a = I^2 R_a$	Ohm's Law

The terms in the above and following equations are listed in Table 1.

These equations may be solved to give:

$$S = \frac{E_o\ \eta^*\ 4\ G\ I + n\eta^*\ 4\ G\ I^2}{\pi d^2\ H} \qquad (1)$$

Table 1. Definitions of Welding Terms

H	=	heat input per unit length (J/mm)
E	=	arc voltage - contact tip to workpiece (V)
I	=	current (A)
η^*	=	overall heat transfer efficiency
R	=	welding speed (mm/s)
S	=	wire feed speed (mm/s)
A_w	=	wire diameter (mm)
E_o	=	open circuit voltage (V)
n	=	volt/amp slope of power supply (V/A) (-0.0307 V/A)
V_w	=	voltage drop across wire length (V)
V_a	=	voltage drop across length of welding arc (V)
δ	=	average wire density (gm/mm^3)
η'	=	fraction of total power transferred from anode spot to solid wire
H_m	=	heat required to melt wire (J/gm)
CTBMD	=	contact tip to base metal distance (mm)

and

$$R = \frac{S \pi d^2}{4G} \tag{2}$$

The current (I) is given by:

$$I = \frac{E_o \pm \sqrt{E_o^2 + 4 \left[n - (1 - \eta') R_a\right] S\pi \frac{d^2}{4} \bar{\delta} \left(\int_{T_{RT}}^{T_m} C_p \, dT + h_f\right)}}{\left[2 (1 - \eta') R_a - n\right]} \tag{3}$$

Two terms in equation (3) proved to be difficult to evaluate: R_a, the resistance of the arc, and n', the efficiency of heat transfer from the arc to the electrode wire. In addition, equations (1)-(3) must be solved iteratively, which proved to be very time consuming for controlling the welding hardware with the computer used. As an alternative method, equation (3) was replaced with an empirical relationship for I, which was derived using a statistical program, SAS[2]. This program calculates a best-fit curve for a set of data:

$$I = C_0 + C_1 \cdot CT + C_2 \cdot E_o + C_3 \cdot I + C_4 \cdot CT \cdot E_o$$

where the C terms are derived constants.

A feedback control scheme was developed to control heat input and reinforcement area by measuring the current. Referring to Figure 1, the desired reinforcement area and heat input are used as input to the model, along with the other welding parameters. The actual welding current is measured and compared to the value predicted by the model, and the difference is used to change the model. The welding speed is simultaneously adjusted to maintain the correct reinforcement area and heat input. In the block diagram (Figure 1), only the top feedback loop is presently implemented.

Welding trials in this work using the model to control reinforcement area and heat input were made using 0.89 mm diameter type E70S-6 wire, with 98% Ar-2% O_2 shielding gas, on 12.7 mm thick type A-36 steel plate in a bead-on-plate configuration. The contact-tip to work piece distance was maintained constant at 15.9 mm and the power supply open circuit voltage was 32 V. All welding involved spray transfer of the molten electrode wire material to the weld pool.

The accuracy of the system has been demonstrated by measuring reinforcement areas and calculated heat inputs obtained during welding for various machine settings[1]. The reinforcement areas are within ±5% of the desired values, the heat inputs are well within ±1% of the desired values. The reinforcement areas were measured from macrophotographs of transverse weld sections using an image digitizing program. The heat inputs were calculated from current, voltage, and travel speed values by the control computer during welding, and assuming a 75% heat transfer efficiency.

To bridge the gap between the control of heat and mass input to the weld and sensing of such factors as weld bead cooling rate and geometry, it is necessary to develop suitable strategies for selecting the desired weldment heat and mass input. These strategies will be based to a great extent on the development of process maps as shown in Figure 2. In Figure 2, the number of weld passes required to fill a certain (arbitrary) weld joint configuration, and the material heat input limits (for HY-130 material) have been superimposed over the spray transfer region for a given voltage and initial contact-tip to workpiece distance. Extending this information over a sufficient range in four dimensions (heat input, mass input, voltage, contact-tip-to workpiece distance) results in a description of the allowed process operating space. Adding pulsed current capability (high current level and time, low current level and time) adds additional complexity.

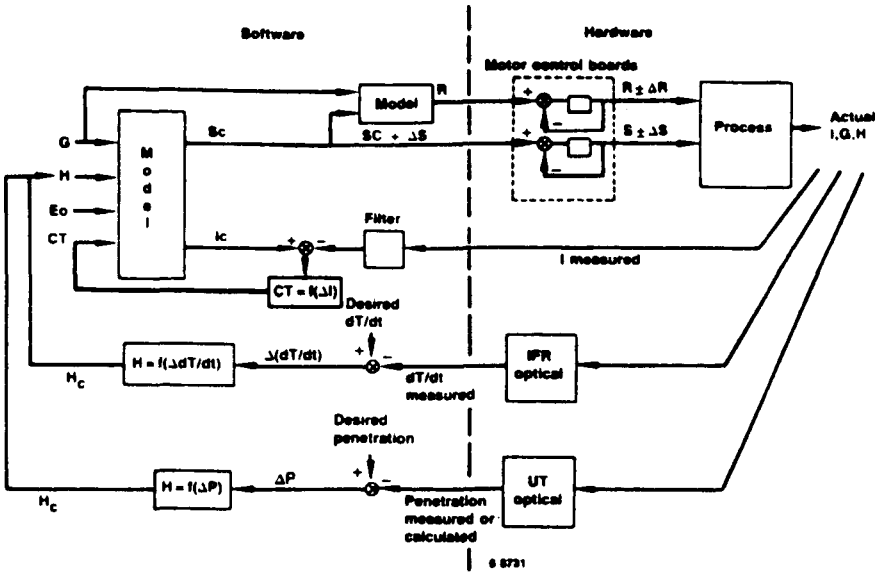

Figure 1. Automated welding control block diagram.

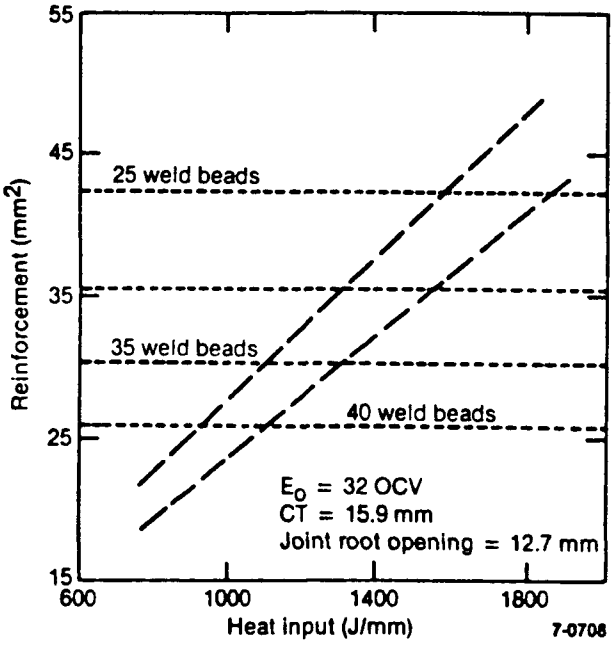

Figure 2. Map of GMA process.

Weld Bead Cooling Rate and Fracture Toughness

Fracture toughness depends on weld bead cooling rate.[3] The feasibility of controlling weld bead cooling rate in real time, independent of the reinforcement area, was examined using a set of welds made at heat inputs from 1050 to 1500 J/mm using reinforcement areas in the range of 30 to 40 mm^2.[1] The weld bead cooling rates were measured by plunging thermocouples into the weld pool at the top center of the weld bead. Although the range of values included in this study is limited, it is clear that the weld bead cooling rate is related to the heat input. Future work on this problem will involve real time measurement of the weld bead cooling rate with an infrared camera in a manner similar to Lukens and Morris[3], and direct closed-loop control of the cooling rate with the error in cooling rate being used to signify the required change in weld bead heat input. Implementation of this scheme is shown as the second feedback line of Figure 1.

Weld Vision System

Electro-optical techniques are used for the indirect measurement of penetration. These techniques are attractive because contact with the workpiece can be avoided and problems with physical wear and heat transfer to the sensor are thereby minimized. Such systems can also accommodate a variety of weld joints and bead geometries by use of adaptive image processing, etc. On the negative side, one can expect optical systems to be relatively intolerant of smoke or aerosol generation at the weld site and to liquid metal spatter. However, a variety of schemes are available to deal with these problems, including the use of a purge gas in the optical path, the use of mechanical shields, and positioning optical surfaces at an appropriate distance to achieve significant cooling of incident spatter.

In 1982, the INEL began exploratory work on the use of machine vision for electric arc welding. Earlier work revealed that the welding arc light is a very severe impediment to formation of good imagery and must be suppressed and/or replaced by illumination from an external light source. Figure 3 is a simple schematic of the experimental arrangement. The goal is to obtain enough peak optical power from the xenon flash lamp to overwhelm the welding arc emission during the brief 2-3 μs interval of the flash. A video camera system equipped with an image intensifier tube is used in a time-gated mode as a very high speed electro-optical shutter. The shutter is synchronized with the flash lamp and therefore acts to accept most of the flash energy reflected from the weld site, but at the same time accepts only a very small fraction of the continuous emission from the welding arc. The synchronized flash and shutter are driven at 30 pulses per second to yield a single flash exposure per video frame.

These early experiments were done with a small gas tungsten arc (GTA) welder operating at 60 to 70 A arc current on stainless steel. Using this system, the visibility through the arc is greatly enhanced, with the weld pool in black contrasting sharply with the solid material in grey. The pool appears black because the liquid metal surface is a very good specular reflector and the xenon flash energy, which is incident from the right, is reflected directionally to the left and not into the video camera field of view. The important result is a quality, high-contrast, video image that can be interfaced with a digital image processing system to automatically characterize the welding pool geometry and geometrical relationship between pool, electrode, and seam.

To improve system performance, a variety of pulsed laser systems were studied as candidates to replace xenon flash illumination, and the nitrogen laser was selected

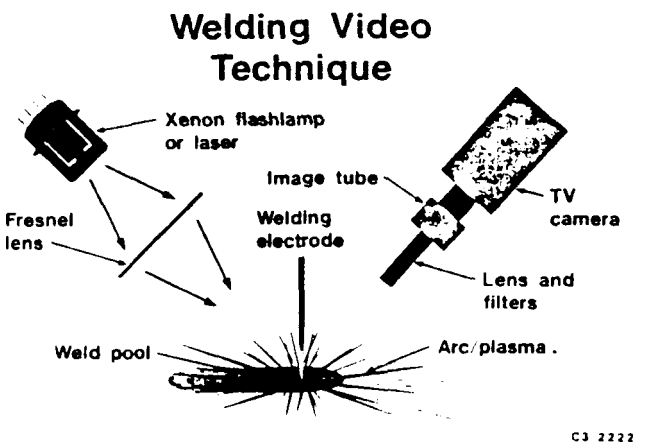

Figure 3. Schematic of weld vision system.

for its relatively high reliability and reasonable price. A pulsed laser is attractive for this application because of the very intense peak optical power levels achievable, the single-wavelength emission which allows the use of narrow band spectral filtering, and the very good focusing characteristics of the beam, which allows transfer of the light energy to the torch via optical fiber.

The nitrogen laser radiates in the near ultraviolet region at 337 nm which does not overlap significant emission lines of the shield gases or alloy materials used in arc welding. This wavelength seems to be suitable in this respect for all welding experiments done to date. Figure 4 shows GMA welding of heavy-section aluminum alloy plate. In this process the shield gas is pure argon and aluminum wire is used as a consumable electrode in place of the tungsten electrode used in the GTA process. The welding current was ~400 A and the weld bead was ~29 mm wide in a flat-bottom V groove. The typical video picture without laser or shuttering is shown in Figure 4a. Some evidence of the wire electrode can be seen below the rim of the gas cup, but little detail can be seen in the groove. The bright elliptical area represents the arc light surrounded by a large depression in the welding pool. A great deal more detail can be seen with laser illumination (Figure 4b).

The camera is presently being used to measure weld pool widths and help understand factors governing weld pool surface characteristics. A technique is being developed that will allow the topographical features of a molten weld pool to be measured.[4] This method capitalizes on the fact that the weld pool is essentially a mirror surface which reflects a distorted image of the weld pool surface. The amount of distortion (topographical change) is measured by comparing the distorted reflection of a known pattern of holes in an aperture array with the undistorted image reflected from a flat mirror. Images of the aperture plate pattern are recorded on video tape, using the weld pool surface as a mirror. This pool has a complex and continuously changing contour, which is due to phenomena such as convection currents and surface tension gradients. The data are then analyzed using a complex mathematical formulation assessing the weld pool topography. Presently, this work is limited to gas tungsten arc welding (GTAW).

Ultrasonic Sensing of Weld Pool Penetration

In contrast to sensing the surface of the weld pool using electro-optical methods, ultrasonic sensing uses sound waves to "look" at the interior of opaque materials. A transducer operating in the pulse-echo mode converts electrical signals into high-frequency sound waves that travel to the area of the weld pool. When the sound wave strikes the metal/molten metal interface, a portion of the energy in the wave is reflected. Some of the reflected sound energy may find its way back to the transducer, which converts the reflected sound into an electrical signal that can be observed on an oscilloscope or digitized by an analog-to-digital converter for computer analysis. This ultrasonic echo provides information about the location of the interface.

The current welding research involves positioning a transducer on the topside of a weld sample, ultrasonically sensing defects 330 mm behind the welding torch in the solidified weld metal, and analyzing the digitized data using pattern recognition techniques.[5] The real-time monitoring system for detecting the molten weld pool uses a 5 MHz contact transducer mounted on various lucite wedges to generate refracted ultrasonic beams in carbon steel. A fixture design allows the transducer, mounted on the lucite wedge, to move along the plate parallel to the weld preparation in alignment with the welding torch (Figure 5). Carbon steel 25.4 mm thick is used in two weld geometries--a single bevel V-groove having a 30° included angle, a 4.76 mm root opening, and a 6.35 mm backup bar; and a V-groove having a 60° included angle, a 4.76 mm root opening, and a 6.35 mm backup bar. Ultrasonic data is

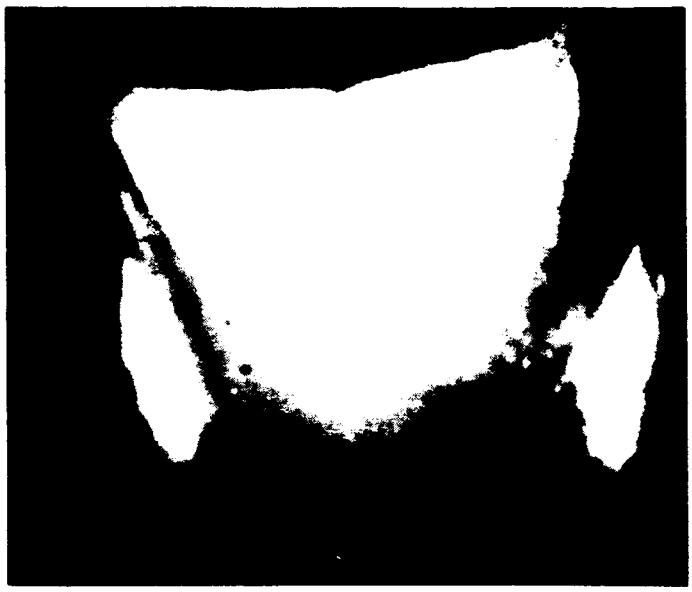

Figure 4a. GMA welding of aluminum without laser illumination.

Figure 4b. Same process using laser illumination and shadows to reveal groove profile.

collected using either a video system which records the real-time ultrasonic signal displayed on the oscilloscope or a DEC LSI 11-23 computer to digitize and store the amplified ultrasonic signal.

Using the transducer fixture and the encoder mounted on the side beam welder, alignment is established between the torch and transducer. Data have been acquired using various lucite wedges which provide different angles of refraction and modes of sound propagation in the weld sample to sense the molten weld pool. A 45° refracted longitudinal sound wave allows sensing of the molten weld pool interior since longitudinal sound waves propagate in the liquid metal. This sensing technique can detect a good weld, porosity in the pool, and lack of side wall penetration on the side of the weld nearest the transducer. A 60° refracted shear wave on a 30° bevel plate allows sensing of the molten-solid interface (shear waves are not

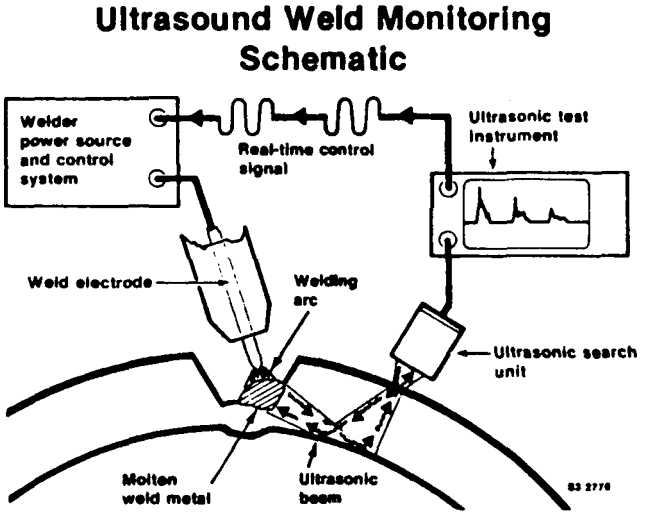

Figure 5. Ultrasound weld monitoring schematic.

supported in liquid) and amount of side wall penetration. The 60° refracted angle is not optimum for sound reflection at the molten/solid interface; however, it is valuable in determining if there is full side wall penetration.

An evaluation process is currently under way using the 45° refracted shear wave data. Reflectors seen before, during, and after welding are evaluated using machined samples to simulate these three unique points of the welding process. Initial correlations between the machined samples and the acquired data indicate that the geometries of the forming molten/solid interfaces can be detected and grouped into several basic geometry types. This information provides the potential of monitoring the interface and providing control input which can assure an optimum interface geometry throughout a welding pass.

CONCLUSION

Process sensing and control of automated welding is possible for the selected parameters discussed above. The success of this integrated control scheme can result in improved weld quality, increased productivity, and energy cost savings in appropriate welding applications.

ACKNOWLEDGMENTS

This work is supported by the U. S. Department of Energy, Office of Energy Research, Office of Basic Engineering Sciences under DOE Contract No. DE-AC07-76ID01570. Appreciation is expressed to U. S. Wallace, C. L. Shull, and C. Stander for technical assistance.

REFERENCES

1. H. B. Smartt, C. J. Einerson, and A. D. Watkins, "Modelling and Control of Gas Metal Arc Welding," in preparation, to be submitted to Welding Journal.
2. SAS Institute, Inc., SAS User's Guide: Statistics, 1982 edition, Cary, NC, SAS Institute, Inc. (1982).
3. W. E. Lukens and R. A. Morris, "Infrared Temperature Sensing of Cooling Rates for Arc Welding Control," Welding Journal, 61, 1, (January 1982), pp. 27-33.
4. R. T. Allemeier and G. D. Lassahn, "Weld Pool Assessment Using Video Data," Proceedings of the 87th AWS Conference (March 1987).
5. J. A. Johnson and N. M. Carlson, "Weld Energy Reduction by Using Concurrent Nondestructive Evaluation," to be published, NDT International (June 1986).